INVESTIGATING THE INTERACTION BETWEEN A HUMAN HEAD AND A SMART HANDSET FOR 4G MOBILE COMMUNICATION SYSTEMS

K. R. Mahmoud, M. El-Adawy, and S. M. M. Ibrahem

Faculty of Engineering
Helwan University
Cairo, Egypt

R. Bansal and K. R. Mahmoud (Visiting)

Department of Electrical and Computer Engineering
University of Connecticut
Storrs, Connecticut, USA

S. H. Zainud-Deen

Faculty of Electronic Engineering
Minufiya University
Menouf, Egypt

Abstract—In this paper we evaluate the potential of a 5-element monopole array incorporated into a handheld device for beamforming in the 5.0-GHz band. The geometry of the handset consists of a 5-element array: four elements located at the handset corners and the fifth-element located at the center. Also, the interaction of the antenna array, mounted on a mobile handset, with a human head phantom is investigated. Firstly, the spatial peak specific absorption rate (SAR) values of 5-element array antennas for mobile handsets in the vicinity of a spherical phantom of a human head are evaluated numerically as a function of the distance between the handset and the head phantom for two different scenarios. Next, the effect of the human head on the handset radiation pattern is studied. The effect of different handset positions on the radiation pattern is also considered. The particle swarm optimization (PSO) algorithm is used to optimize the complex excitations of the adaptive arrays elements in a mutual coupling environment for beamforming synthesis. All numerical simulations are performed using the FEKO Suite 5.3

software. To validate the numerical simulations, we first perform two validation tests and compare the numerical results with published simulated and measurement results.

1. INTRODUCTION

The approaching 4G (fourth generation) mobile cellular systems are projected to solve still-remaining problems of 3G (third generation) systems and to provide a wide variety of new services, from high quality voice to high definition video to high-data-rate wireless channels. The most promising frequency band for these systems is the 4–5 GHz band because of spectrum availability, wide-area coverage, mobility, and the relatively low cost for the associated RF equipment [1].

Since antennas for mobile handsets are often used in the vicinity of the human body, the electromagnetic wave radiated by the antennas is partly absorbed by the human body. Regulations and standards have been issued to limit the radiation exposure from the mobile handsets. The exposure guideline employs a unit known as the Specific Absorption Rate (SAR). The SAR quantifies the power absorbed per unit mass of tissue. This quantity is defined as:

$$SAR = \frac{\sigma}{2\rho} |E_i|^2 \tag{1}$$

where E_i is the max value of the electric field strength in the tissue in V/m, σ is the conductivity of body tissue in S/m, and ρ is the density of body tissue in kg/m^3. The SAR limit specified in IEEE C95.1: 2005 has been updated to 2 W/kg over any 10-g of tissue [2]. This new SAR limit specified in IEEE C95.1: 2005 is comparable to the limit specified in the International Commission on Non-Ionizing Radiation Protection (ICNIRP) guidelines [3]. It is important to investigate the SAR value produced by the radiation from the mobile handsets in designing antennas for mobile handsets.

Many studies on the SAR value of a single antenna for mobile handsets have been carried out in different frequency bands [4–17]. Since the use of adaptive array antennas is one of the most effective ways of increasing the spectral efficiency and improving the communication quality in the mobile communication system, a great deal of attention has turned to how to design antenna arrays on mobile handsets to meet the needs of significantly higher bit-rates for the next-generation wireless communications [18–21]. An investigation of the SAR caused by antenna arrays at 1.9 GHz has been reported and it was shown that the SAR value reaches a maximum when the phase

difference is near 180 degrees and a minimum when the phase difference is approximately 0 degree [21]. However, sufficient attention has not yet been paid to antenna arrays for mobile handsets especially in the 5.0 GHz band. In addition, few papers considered the effect on SAR when smart antennas are introduced at the handset.

The effect of the human head on the accuracy and depth of adaptive nulling for a linear dipole array at 5.0 GHz band is investigated in [22]. This effect is dependent on the separation between the array and the head. A metallic plate is inserted between the array and the head to suppress this effect. In [23] the peak SAR value at 2 GHz and 5 GHz is evaluated numerically as a function of the distance between the array antenna and a spherical head model when the two elements of an antenna array are voltage-fed cophase or reverse-phase.

A study of how the SAR is affected by different shapes and electrical properties of the human head exposed to a cellular phone has been reported [24]. The results showed that the shape of the human head plays a minor role in calculating the SAR induced in human-head models. In [25], the effect of the human head heterogeneity and shape on the radiation characteristics of dipole antennas have been discussed at 5.0 GHz band. It was found that the input impedance and the radiation pattern of the dipole antenna are not sensitive to the heterogeneity and the shape of the head model. Therefore, in this paper, a simplified homogeneous spherical head model is used.

In the array pattern synthesis, the objective function and the constraints are often highly nonlinear and nondifferentiable. Therefore, analytical methods, such as the Taylor method and the Chebyshev method, are not applicable any more. Rather, stochastic methods are necessary to deal efficiently with large nonlinear search spaces. Compared with other evolutionary algorithms such as the genetic algorithm (GA), the particle swarm optimization (PSO) algorithm is much easier to implement and requires minimum mathematical processing. Therefore, in this paper the PSO is used to adjust the relative phase shifts and the amplitudes of the excitations of the array elements for beam synthesis in a mutual coupling environment. In particular, we evaluate the potential of a 5-element monopole array incorporated into a handheld device for beamforming in the 5.0-GHz band. The geometry of the handset consists of a 5-element array: four elements located at the handset corners and the fifth-element located at the center. Also, the interaction of the antenna array, mounted on a mobile handset, with a human head phantom is investigated. First, the spatial-peak specific absorption rate (SAR) values of 5-element array antennas for mobile handsets in the vicinity of a spherical phantom of a human head are evaluated numerically as a function of the distance

between the handset and the head phantom for two different scenarios. In addition, the effect of the human head on the handset radiation pattern will be considered. Then the effect of locating the handset in different positions on the radiation pattern is studied. The total power delivered to all antenna arrays for all cases is held constant (100 mW). All numerical simulations are performed using the FEKO Suite 5.3 software. The core of the FEKO programs is based on the method of moments (MoM).

The organization of the present paper is as follows. In Section 2, a brief introduction to the particle swarm optimization algorithm is presented. In Section 3, the validation of the numerical simulations is presented. Handset design and simulation results are discussed in Section 4. The interaction between the handset and the human head is investigated in Section 5. In Section 6, the effect of moving the handset position in different directions is studied. Finally, Section 7 presents the conclusions.

2. PARTICLE SWARM OPTIMIZATION (PSO) ALGORITHM

PSO is a population based optimization tool, where the system is initialized with a population of random particles and the algorithm searches for optima by updating generations [26]. Suppose that the search space is D-dimensional. The current position of the i-th particle can be represented by a D-dimensional vector $X_i = (x_{i1}, x_{i2}, \ldots, x_{iD})$ and the velocity of this particle is $V_i = (v_{i1}, v_{i2}, \ldots, v_{iD})$. The best previously visited position of the i-th particle is represented by $P_i = (p_{i1}, p_{i2}, \ldots, p_{iD})$ and the global best position of the swarm found so far is denoted by $P_g = (p_{g1}, p_{g2}, \ldots, p_{gD})$. The fitness of each particle can be evaluated through putting its position into a designated objective function. The particle's velocity and its new position are updated as follows:

$$v_{id}^{k+1} = \omega v_{id}^k + c_1 r_1^k \left(p_{id}^k - x_{id}^k \right) + c_2 r_2^k \left(p_{gd}^k - x_{id}^k \right) \tag{2}$$

$$x_{id}^{k+1} = x_{id}^k + v_{id}^{k+1} \Delta t \tag{3}$$

where $d \in \{1, 2, \ldots, D\}$, $i \in \{1, 2, \ldots, N\}$, N is the population size, the superscript k denotes the iteration number, ω is the inertia weight, r_1 and r_2 are two random values in the range $[0, 1]$, c_1 and c_2 are the cognitive and social scaling parameters which are positive constants ($c_1 = 2.8$ and $c_2 = 1.3$). In this paper, the PSO algorithm is employed with a population size of 20 and 500 iterations. For beamforming

synthesis, the amplitude was allowed to vary between 1.0 and 3.0 and the phase was allowed to vary between $-\pi$ and π.

A very simple objective function for the antenna array is used for maximizing the output field toward the desired signal at φ_i and minimizing the total output field in the direction of the interfering signals at φ_j.

$$Objective\_function = \sum_{i=1}^{N} a_i \left|E_\theta(\varphi_i)\right| - \sum_{j=1}^{M} b_j \left|E_\theta(\varphi_j)\right| \quad (4)$$

where E_θ is the vertical field component and the constants a_i and b_j are the weights that control the contribution from each term to the overall objective function. The emphasis on E_θ is related to using vertical monopole-elements in our design. The constants N and M represent the number of desired signals and interferers respectively. In our analysis, we take the weights $a_i = 2$ and $b_j = 1$ to give some priority to maximizing the output field toward the desired signal rather than minimizing the output field in the direction of the interfering signals.

3. VALIDATION OF NUMERICAL SIMULATIONS

To verify the numerical simulations we first perform two validation tests and compare their results with published computed and measured results. The first example is for handset modeling while the second one is for the SAR simulation. In the first validation example test, the cellular phone was modeled as a metallic box (perfect conductor), having external dimensions $1.31 \times 5.25 \times 15.1$ cm. The monopole antenna was modeled by a $\lambda/4$ metallic wire fixed on top of the metal box [4]. Figure 1 shows a comparison between the resulting values of $|S_{11}|$ employing the MoM-based Feko technique and the results obtained via the FDTD technique and the measurements from reference [4]. It can be seen that our numerical simulation results are in good agreement with the published simulated and measured results. In the second example, as shown in Figure 2, a spherical head phantom is irradiated by a half-wave dipole antenna at 835 MHz in the measurement setup [27]. The dipole length is 178 mm and it is placed at several distances from the outer surface of the sphere. The phantom consists of an outer glass shell and the head tissue-equivalent material. The inner diameter and the thickness of the glass shell are 213 mm and 5 mm, respectively. Electrical properties of the glass shell and the head tissue-equivalent material are shown in Table 1. Table 2 compares the measured and simulated peak 1-g SAR for three different distances d between the radiating dipole and the phantom [16, 27]. The SAR quantity reported in Table 2 is normalized to the output

power of 0.5 W. The output power is sum of the absorbed power in the human body and the radiated power. As shown in Table 2, numerical simulation results are in good agreement with the measured data.
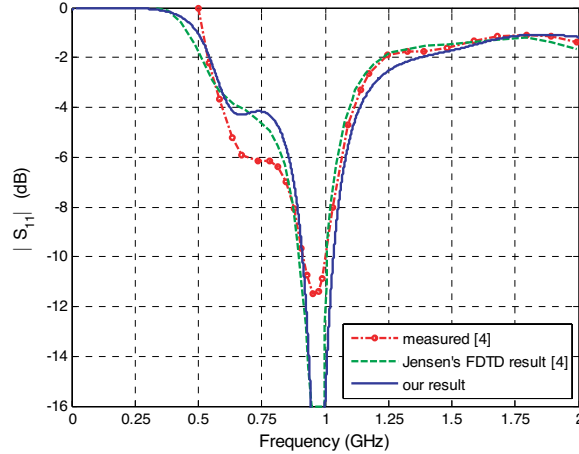
Figure 1. Comparison between the resulting values of $|S_{11}|$ and the results obtained via FDTD technique and the measurements in reference [4] for the $\lambda/4$ monopole on a PEC handset model.

Table 1. Properties of the spherical head phantom used for validation test [27]. (ε_r = relative permittivity and σ = conductivity.)

Frequency	Glass shell		Tissue-equivalent material	
	ε_r	σ	ε_r	σ
835 MHz	4	0	41.1	1.06

Table 2. Comparison of measurement [27] and simulation results [16, 27] for peak 1-g SAR in head equivalent liquid (Figure 1).

d (mm)	Peak 1-g SAR (W/kg)			
	measured [27]	Simulated [27]	Simulated [16]	our results
5	6.78	6.77	7.27	6.796
15	3.41	3.27	3.24	3.337
25	1.85	1.68	1.65	1.821
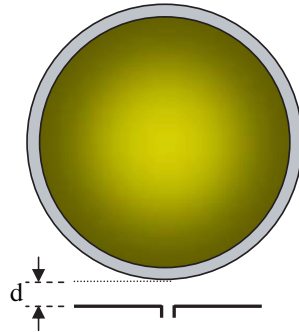
Figure 2. Exposure of a spherical head phantom by a half-wave dipole antenna.

4. HANDSET DESIGN AND SIMULATION RESULTS

In this paper, the handset has been modeled as a metallic box with the dimensions $46.4 \times 16.4 \times 96.4$ mm. These dimensions are large enough to let us design the array with a $\lambda/4$ spacing without making the overall size too large. The monopole antennas were modeled by $\lambda/4$ metallic wires fixed on top of the metal box and fed with voltage sources. The geometry consists of a 5-element array of $\lambda/4$ monopoles; four elements located at handset corners and the fifth-element located at the center as shown in Figure 3. The monopoles were chosen to be of radius 0.2 mm. The metal box with the attached monopoles is covered with a dielectric material ($\varepsilon_r = 2.1$), having external dimensions $50 \times 20 \times 114.7$ mm. The total power delivered to all antenna arrays for all cases is held constant (100 mW).

As an example of adaptive beamforming, we considered two scenarios as shown in Table 3. Figure 4 shows the capability of the 5-element array geometry to achieve both scenarios 1 and 2. The required amplitude and phase excitations of each element to obtain the beampatterns in Figure 4 are shown in Table 4.

Table 3. Descriptions of the environmental scenarios.

Scenario #1				Scenario #2			
Desired	*Interference*			*Desired*	*Interference*		
0°	90°	180°	270°	90°	0°	180°	270°
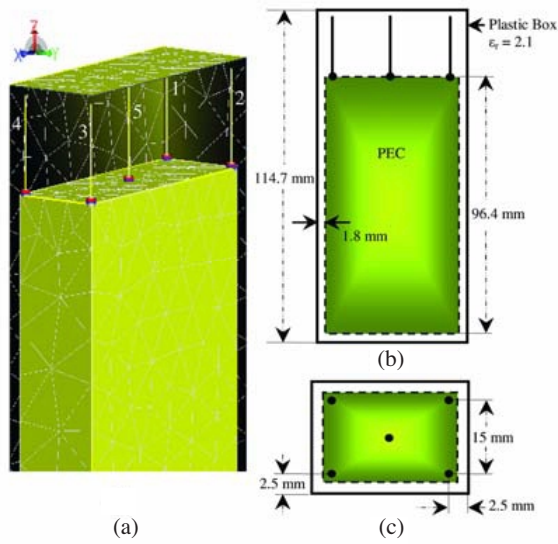
Figure 3. Geometry of the five-element monopole array mounted on the mobile handset. (a) Numerical model, (b) Elevation view, (c) Top view.
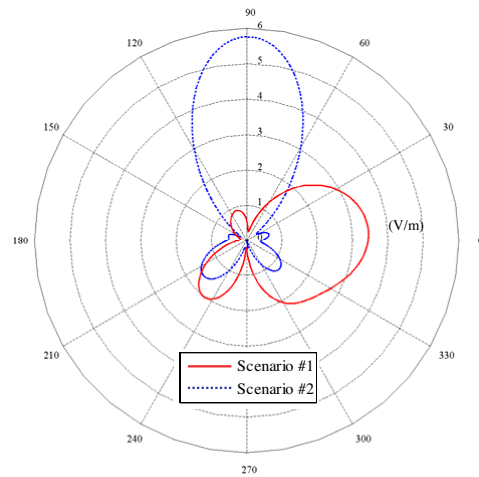
Figure 4. The radiation pattern $|E_\theta|$ for the five-element monopole array mounted on the mobile handset.

(a)   (b)
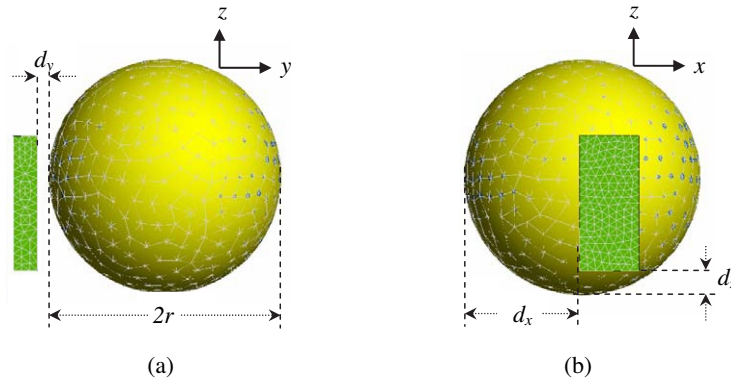
Figure 5. Homogeneous human head model and handset configuration. (a) Front view, (b) Side view.

Table 4. The required amplitude and phase excitations of each element for 5-element monopole array on handset.

Element	*Scenario #1*		*Scenario #2*	
No.	*amplitude*	*phase*	*amplitude*	*phase*
1	2.87	$-17.45°$	1.23	$22.91°$
2	2.56	$0.92°$	1.95	$-119.03°$
3	1.29	$-70.74°$	2.05	$-125.33°$
4	1.41	$99.88°$	1.28	$25.61°$
5	1.96	$-171.89°$	2.91	$-29.09°$

5. INTERACTION BETWEEN HANDSET AND HUMAN HEAD

In this section, the interaction between the mobile handset and the human head has been studied. A simplified homogeneous spherical head model is used. The sphere had a radius of $r = 10$ cm and the tissue that it contained had a relative permittivity of $\varepsilon_r = 33.5$ and conductivity $\sigma = 2.8$ S/m. These tissue-equivalent dielectric parameters were chosen according to [28] for simulating brain tissue at 5 GHz. For the computation of SAR, the head tissue density is assumed to be 1000 kg/m^3. The relative position of the handset relative to human head model is illustrated in Figure 5. The interaction between the mobile handset and the human head is studied from two viewpoints:

the impact of the handset on SAR and the effect of the human head on the radiation pattern.

5.1. The Impact of the Handset on SAR

Now, all newly proposed handset antennas consider SAR an important design specification that they must meet. Therefore, in this section we study the impact of the handset on SAR. Figures 6 shows the variation of the spatial-peak SAR over 10-g of tissue with respect to the distance d_y between the handset and the outer surface of the homogeneous human head phantom for $d_x = 10$ cm and $d_z = 2$ cm. The first case is for a single-monopole element modeled by a $\lambda/4$ metallic wire fixed at the center of the metal box. Case 2 is the 5-element monopole array incorporated into the handheld device but all elements are excited with the same amplitude and phase $(2, 0°)$. Cases 3 and 4 are the same design as in Case 2 but the monopole elements are fed to achieve scenarios 1 and 2, respectively, as in Section 4. It should be noted that Case 4 is the worst case where the desired SOI is in the direction of the human head (the human head is located between the handset and the base station).

This figure underscores several points. A first observation from this plot is that dividing the delivered power in one antenna into five antennas dose not significantly increase the spatial-peak SAR especially if these elements are excited with the same amplitude and phase. But if these array elements are fed with different voltage values to achieve a certain scenario, the spatial-peak SAR is affected significantly. The results obtained in Figure 6 indicate that, the resulting SAR values for the smart handset in different scenarios are under the limits set by IEEE C95.1: 2005 or ICNIRP standards. In addition, some other issues should be noted as well, as suggested by a comparison of the SARs induced in the realistic human-head model for the homogeneous and the inhomogeneous cases [24]. It is found that the constitutive parameters of a human head significantly affect the result of the SAR induced in homogeneous or inhomogeneous head models where the local maximum SAR induced in the homogeneous human-head model is larger than that induced in the inhomogeneous human head model. That means that the simulated SAR values in this paper conservative estimates for the inhomogeneous human head model.
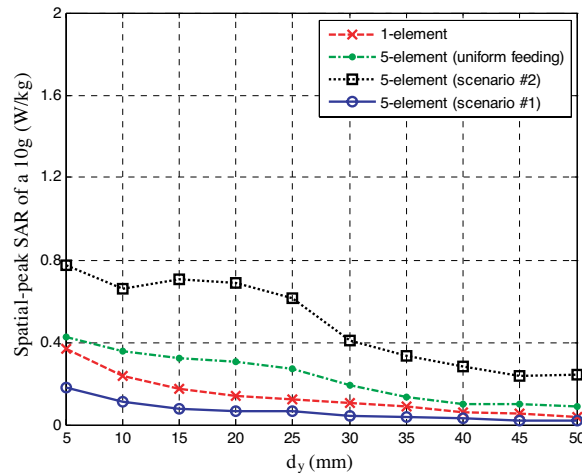
Figure 6. Variation of spatial-peak SAR over 10-g for different distances d_y between handset and outer surface of the homogeneous human head phantom. The handset delivered power is 100 mW.

5.2. The Effect of the Human Head on the Radiation Pattern

In this section we study the effect of the human head on the radiation pattern. Figure 7(a) shows the handset radiation pattern in the presence of a homogeneous human head phantom for scenarios 1 and 2. The distances between the human head model and the handset are fixed to $d_y = 1$ cm, $d_x = 10$ cm and $d_z = 2$ cm. It is noted that, in the case of scenario #1, only a slight effect is observed where the handset is still able to direct most of the field in the desired direction and to minimize it in the interference directions. But for scenario #2, where the maximum field is directed towards the head, the radiation pattern is greatly affected by the presence of the human head, where some power is already directed to the interference angles. Therefore, we should re-optimize the beampattern in the presence of the head.

Figure 7(b) shows the re-optimized beampattern of the handset in the presence of the homogeneous human head phantom for scenarios 1 and 2, at the same distances. The figure shows the ability of the design to direct the maximum field towards the direction of the SOI while placing deeper nulls towards the angles of SNOIs in the presence of the human head for different scenarios. On the other hand, the SAR is increased where the spatial-peak SAR over 10-g is increased to 0.3775 W/kg and 1.131 W/kg for scenarios 1 and 2 respectively.

(a)   (b)
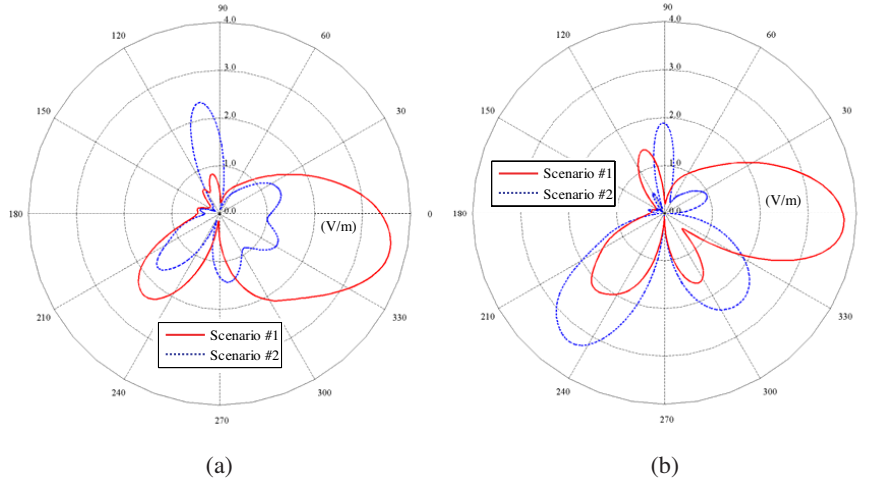
Figure 7. The radiation pattern $|E_\theta|$ of the handset in the presence of the homogeneous human head phantom at distances ($d_y = 1\,\text{cm}$, $d_x = 10\,\text{cm}$ and $d_z = 2\,\text{cm}$). (a) Pre-optimized beampattern, (b) Optimized beampattern.

However, these values of SAR are still under the guideline limitations. Table 5 shows the required amplitude and phase excitations of each element for a 5-element monopole array on a handset to obtain the beampatterns in Figure 7(b).

Table 5. The required amplitude and phase excitations of each element for the 5-element monopole array on a handset in the presence of the homogeneous human head model at distances $d_y = 1\,\text{cm}$, $d_x = 10\,\text{cm}$ and $d_z = 2\,\text{cm}$.

Element	*Scenario #1*		*Scenario #2*	
No.	*amplitude*	*phase*	*amplitude*	*phase*
1	2.69	78.58°	1.85	129.69°
2	1.07	169.33°	2.69	−23.16°
3	1.65	94.19°	1.58	−136.16°
4	1.89	−101.26°	1.41	−9.79°
5	2.91	−110.43°	1.58	76.13°

6. THE EFFECT OF CHANGING THE SMART HANDSET POSITION

In this section we study how the radiation pattern is affected by changing the position of the handset either in the y-direction (forward and back) or in the x-direction (right and left) or in z-direction (up and down) relative to the human head. Also, we study the best way to re-optimize the beampattern in the new position. To illustrate this effect we take into account the worst case (scenario #2). The original case is the optimized beampattern at the distances $d_y = 1$ cm, $d_x = 10$ cm and $d_z = 2$ cm shown in Figure 7(a). The required amplitude and phase excitations are already shown in Table 5. This study is presented in three subsections introducing the effect of changing the distances d_y, d_x and d_z.

6.1. The Effect of Changing the Distance (d_y)

In this part, we will study the effect of changing the distance d_y on the optimized beampattern. Figure 8 shows the radiation patterns for different values of d_y, 5 mm, 15 mm and 20 mm, respectively. It is found that, for distances 5 mm and 15 mm, still acceptable beampatterns are obtained. However, at a distance of $d_y = 20$ mm, some of the power is directed toward the nulls. Therefore, the handset should re-optimize the feedings to obtain an acceptable beampattern. We will re-optimize the beampattern using a lower number of iterations ($k = 200$).

Two cases are considered to re-optimize the beampattern. First, we re-optimized the beampattern where the 5-element monopole array is excited with the same amplitude and phase (2, 0°) as an initial iteration. In the other case, we will re-optimize the beampattern using the previous amplitude and phase excitations shown in Table 5 as an initial iteration. The resultant radiation patterns for these cases are shown in Figure 9. As a comparison between the obtained beampatterns we note that, a slightly better result is obtained by using the previous excitation values as an initial iteration. That means we can use a smaller number of iterations for each handset position change, which will save the required time to optimize the beampattern. Therefore, this case (case #2) will be used in the following subsections to re-optimize the beampatterns.

6.2. The Effect of Changing the Distance (d_x)

Now, we study the effect of changing the distance d_x on the optimized beampattern. Figure 10 shows the radiation pattern of the handset when it moved back and forward (y-direction) for different distances.
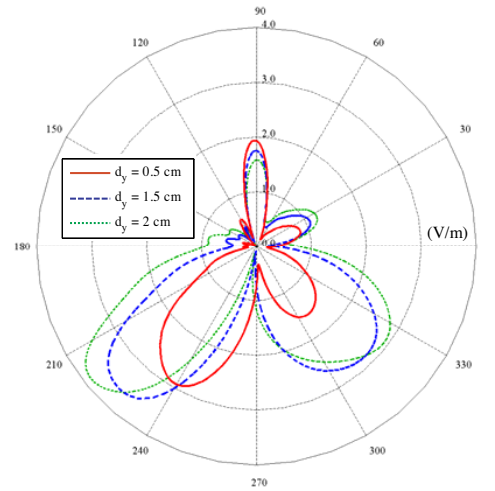
Figure 8. The radiation pattern $|E_\theta|$ of the handset in the presence of the human head for different distances of d_y where $d_x = 10$ cm and $d_z = 2$ cm.
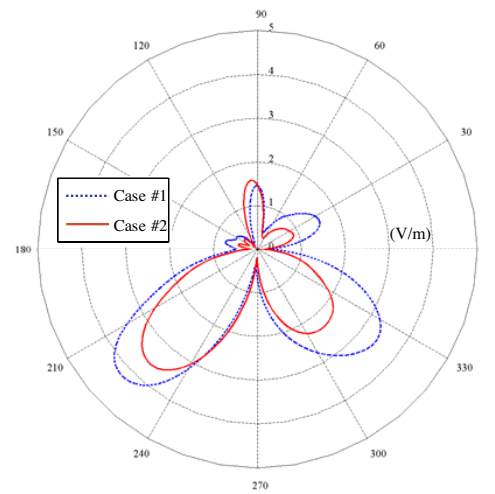
Figure 9. The optimized radiation pattern $|E_\theta|$ of the handset in the presence of the human head at distances ($d_y = 2$ cm, $d_x = 10$ cm and $d_z = 2$ cm). Cases 1 and 2 are based on re-optimizing the beampattern by exciting the elements with the same amplitude and phase $(2, 0°)$ or exciting the elements with the previous [Table 5] amplitude and phase, respectively, for the first iteration.
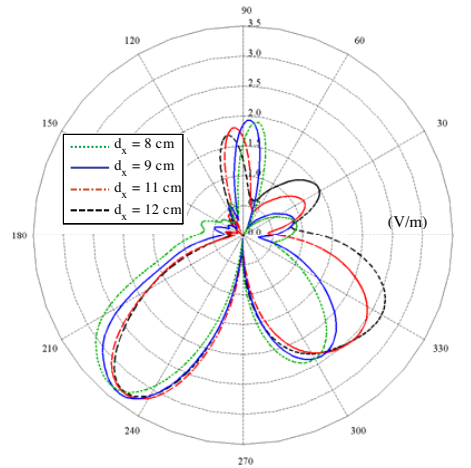
Figure 10. The radiation pattern $|E_\theta|$ of the handset in the presence of the human head for different distances of d_x where $d_y = 1$ cm and $d_z = 2$ cm.

It is found that if the handset is shifted by ± 1 cm, acceptable beampattern is still obtained. However, at the same distances ($d_y = 1$ cm and $d_z = 2$ cm), with deviating the handset by $d_x = \pm 2$ cm we note that some of the power is directed toward the nulls. Therefore, the handset should re-optimize the feedings to obtain an acceptable beampattern. Figure 11 shows the optimized beampattern at distances $d_x = 8$ cm and 12 cm.

6.3. The Effect of Changing the Distance (d_z)

Finally, we study the effect of changing the distance d_z on the optimized beampattern. Figure 12 shows the radiation pattern of the handset when it moved up and down (z-direction). Again, it is found that if the handset is shifted by ± 1 cm, an acceptable beampattern is still obtained. However, shifting the handset by $d_z = 2$ cm, some of the power is directed toward the nulls as shown in Figure 12. Therefore, the feedings were re-optimized to obtain an acceptable beampattern. Figure 13 shows the re-optimized beampattern at $d_z = 4$ cm.

It should be noted that better results can be obtained in the previous studies if the number of iterations is increased but then the required processing time will also increase. There are other trade-offs between the required processing time and the accuracy such as letting the feeding excitation (amplitude and phase) to have discrete values.
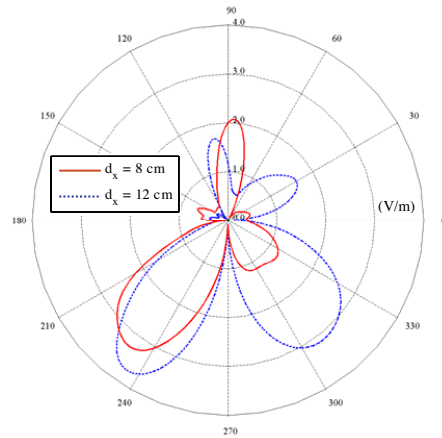
Figure 11. The optimized radiation pattern $|E_\theta|$ of the handset in the presence of the human head at distances ($d_y = 1$ cm and $d_z = 2$ cm).
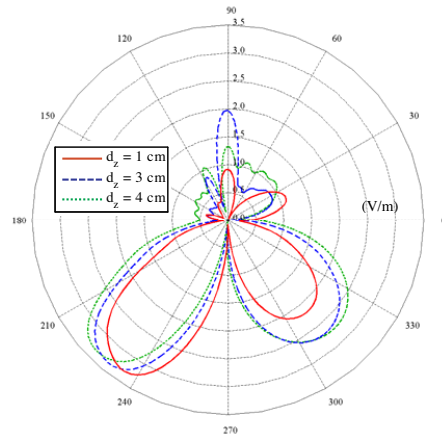
Figure 12. The radiation pattern $|E_\theta|$ of the handset in the presence of the human head for different distances of d_z where $d_y = 1$ cm and $d_x = 10$ cm.

Also, the antenna array may be optimized using only discrete phase-shifters. Clearly if the quantized step size is increased, the required convergence time will decrease; on the other hand, the accuracy will decrease. In addition, a modified version of PSO can be used to get a better convergence rate [29, 30].
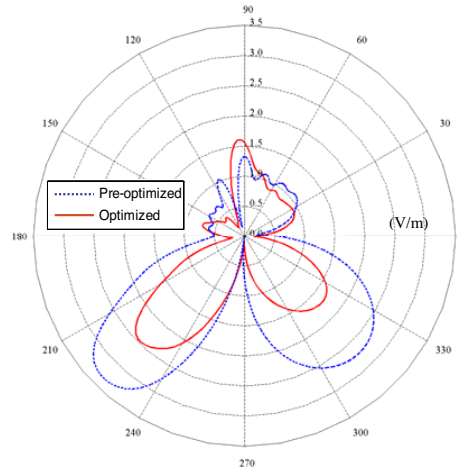
Figure 13. The optimized radiation pattern $|E_\theta|$ of the handset in the presence of the human head at distances ($d_y = 1\,\text{cm}$, $d_x = 10\,\text{cm}$ and $d_z = 4\,\text{cm}$).

7. CONCLUSIONS

In this paper we investigated the capability of a 5-element monopole array into a handheld device for 4G communication systems in the 5.0-GHz band for beamforming synthesis in a mutual coupling environment. Also, the interaction of the antenna array, mounted on a mobile handset, with a human head phantom is investigated. The spatial-peak specific absorption rate (SAR) values of the smart handset in the vicinity of a spherical phantom of a human head are evaluated numerically as a function of the distance between the handset and the head phantom for two different scenarios. It is found that the smart handset can work under SAR guidelines limitations. In addition, the effect of the human head on the handset radiation pattern is studied. Also, the effect of changing the handset position in different directions on the radiation pattern is considered. It is found that if the handset is approximately shifted by $\pm 1\,\text{cm}$ in any direction, an acceptable beampattern is still obtained without the need of re-optimization. The PSO algorithm is used to optimize the complex excitations of the adaptive arrays elements for beamforming. The numerical simulation results demonstrated the feasibility of smart handset beamforming to nullify the effects of interfering sources in the presence of the human head model.

REFERENCES

1. Sun, J., J. Sauvola, and D. Howie, "Features in future: 4G visions from a technical perspective," *Global Telecommunications Conference, 2001. GLOBECOM '01. IEEE*, Vol. 6, 3533–3537, San Antonio, TX, USA, 2001.

2. IEEE C95.1:2005, "Safety levels with respect to human exposure to radio frequency electromagnetic fields, 3 kHz to 300 GHz," IEEE standard, 2005.

3. ICNIRP Guidelines, "Guidelines for limiting exposure to time-varying electric, magnetic, and electromagnetic fields (up to 300 GHz)," *Health Phys.*, Vol. 74, No. 4, 1998.

4. Jensen, M. A. and Y. Rahmat-Samii, "EM interaction of handset antennas and a human in personal communications," *Proceedings of the IEEE*, Vol. 83, No. 1, 1106–1113, January 1995.

5. Vaughan, R. G. and L. S. Neil, "Evaluation of antenna configurations for reduced power absorption in the head," *IEEE Transactions on Vehicular Technology*, Vol. 48, No. 5, 1371–1380, September 1999.

6. Kang, X. K., L. W. Li, M. S. Leong, and P. S. Kooi, "A spheroidal vector wave function analysis of field and SAR distributions in a dielectric prolate spheroidal human head model," *Progress In Electromagnetics Research*, PIER 22, 149–179, 1999.

7. Li, L. W., M. S. Leong, P. S. Kooi, and T. S. Yeo, "Specific absorption rates in human head due to handset antennas: A comparative study using FDTD method," *Journal of Electromagnetic Waves and Applications*, Vol. 14, No. 7, 987–1001, 2000.

8. Kang, X. K., L. W. Li, M. S. Leong, and P. S. Kooi, "A method of moments dtudy of SAR inside dpheroidal human head and current distribution along handset wire antennas," *Journal of Electromagnetic Waves and Applications*, Vol. 15, No. 1, 61–76, 2001.

9. Kouveliotis, N. K., P. J. Papakanellos, E. D. Nanou, N. I. Sakka, V. S. G. Tsiafakis, and C. N. Capsalis, "Correlation between SAR, SWR and distance of a mobile terminal antenna in front of a experimental validation," *Journal of Electromagnetic Waves and Applications*, Vol. 17, No. 11, 1561–1581, 2003.

10. Fung, L. C., S. W. Leung, and K. H. Chan, "Experimental study of SAR reduction on commercial products and shielding materials in mobile phone applications," *Microwave and Optical Technology Letters*, Vol. 36, No. 6, 419–422, March 2003.

11. De Salles, A. A., C. R. Ferndadez, and M. Bonadiman, "FDTD simulations and measurements on planar antennas for mobile phones," *Microwave and Optoelectronics Conference. IMOC 2003. Proceedings of the 2003 SBMO/IEEE MTT-S International*, Vol. 2, 1043–1048, Sept. 2003.

12. Stavros, K. and K. S. Nikita, "Study of the coupling between human head and cellular phone helical antennas," *IEEE Transactions on Electromagnetic Compatibility*, Vol. 46, No. 1, 62–70, February 2004.

13. Kouveliotis, N. K., S. C. Panagiotou, P. K. Varlamos, and C. N. Capsalis, "Theoretical approach of the interaction between a human model and a mobile handset helical antenna using numerical methods," *Progress In Electromagnetics Reasearch*, PIER 65, 309–327, 2006.

14. Klemm, M. and G. Troester, "EM energy absorption in the human body tissues due to UWB antennas," *Progress In Electromagnetics Research*, PIER 62, 261–280, 2006.

15. Ding, W., Y. Zhang, P. Y. Zhu, and C. H. Liang, "Study on electromagnetic problems involving combinations of arbitrarily oriented thin-wire antennas and inhomogeneous dielectric objects with a hybrid MOM-FDTD method," *Journal of Electromagnetic Waves and Applications*, Vol. 20, No. 11, 1519–1533, 2006.

16. Ebrahimi-Ganjeh, M. A. and A. R. Attari, "Interaction of dual band helical and PIFA handset antennas with human head and hand," *Progress In Electromagnetics Reasearch*, PIER 77, 225–242, 2007.

17. Kuo, L.-C., Y.-C. Kan, and H.-R. Chuang, "Analysis of a 900/1800-MHz dual-band gap loop antenna on a handset with proximate head and hand model," *Journal of Electromagnetic Waves and Applications*, Vol. 21, No. 1, 107–122, 2007.

18. Dietrich, Jr., C. B., W. L. Stutzman, B. Kim, and K. Dietze, "Smart antennas in wireless communications: Base-station diversity and handset beamforming," *IEEE Antennas and Propagation Magazine*, Vol. 42, No. 5, 142–151, October 2000.

19. Denidni, T. A., D. McNeil, and G. Y. Delisle, "Experimental investigations of a new adaptive dual-antenna array for handset applications," *IEEE Trans. Veh. Technol.*, Vol. 52, No. 6, 1417–1423, Nov. 2003.

20. Yuan, Q., Q. Chen, and K. Sawaya, "Performance of adaptive array antenna with arbitrary geometry in the presence of mutual coupling," *IEEE Trans. Antennas Propag.*, Vol. 54, No. 7, 1991–1996, July 2006.

21. Chim, K.-C., K. C. L. Chan, and R. D. Murch, "Investigating the impact of smart antennas on SAR," *IEEE Trans. Antennas Propag.*, Vol. 52, No. 5, 1370–1374, May 2004.

22. Akimasa, H., S. Mitsuzono, and T. Shiozawa, "Feasibility study of adaptive nulling on handset for 4G mobile communications," *IEEE Antennas and Wireless Propagation Letters*, Vol. 3, 120–122, 2004.

23. Chen, Q., Y. Komukai, and K. Sawaya, "SAR investigation of array antennas for mobile handsets," *IEICE Trans. Commun.*, Vol. E90-B, No. 6, 1354–1356, June 2007.

24. Chen, H.-Y. and H. Yang, "SAR affected by shapes and electrical properities of the human head exposed to the cellular phone," *Microwave and Optical Technology Letters*, Vol. 42, No. 1, 1–4, July 2004.

25. Yoshida, K., A. Hirata, Z. Kawasaki, and T. Shiozawa, "Human head modeling for modeling for handset antenna design at 5 GHz band," *Journal of Electromagnetic Waves and Applications*, Vol. 19, No. 3, 401–411, 2005.

26. Kennedy, J. and R. Eberhart, "Particle swarm optimization," *IEEE International Conferenceon Neural Networks*, Vol. 4, 1942–1948, Perth, Australia, 1995.

27. Yu, Q. and O. P. Gandhi, "An automated SAR measurement system for compliance testing of personal wireless devices," *IEEE Trans. EMC*, Vol. 41, No. 3, 234–244, 1999.

28. Gabriel, C., "Compilation of the dielectric properties of body tissues at RF and microwave frequencies," Brooks Air Force Technical Report AL/OE-TR-1996-0037, 1996.

29. Mahmoud, K. R., M. El-Adawy, R. Bansal, S. H. Zainud-Deen, and S. M. M. Ibrahem, "A comparison between circular and hexagonal array geometries for smart antenna systems using particle swarm optimization algorithm," *Progress In Electromagnetics Research*, PIER 72, 75–90, 2007.

30. Mahmoud, K. R., M. El-Adawy, R. Bansal, S. H. Zainud-Deen, and S. M. M. Ibrahem, "Analysis of uniform circular arrays for adaptive beamforming applications using particle swarm optimization algorithm," *Int. J. RF Microwave Computed Aided Eng.*, Vol. 18, 42–52, 2008.